

www.acsami.org Research Article

Probing the Origin of Light-Enhanced Ion Diffusion in Halide Perovskites

Angelo D. Marshall,* Jagaran Acharya, Ghadah Alkhalifah, Bhupal Kattel, Wai-Lun Chan,* and Judy Z. Wu*



Cite This: ACS Appl. Mater. Interfaces 2021, 13, 33609-33617



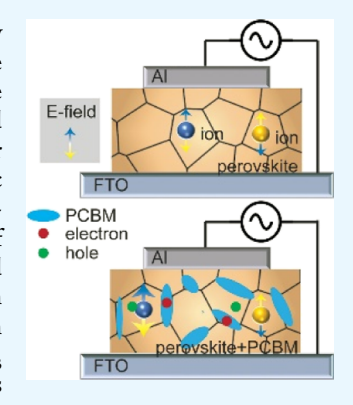
ACCESS

Metrics & More

Article Recommendations

Supporting Information

ABSTRACT: Organic—inorganic hybrid halide perovskites have emerged recently as highly promising materials for optoelectronics such as photovoltaics and photodetectors. A unique feature of these materials is ion diffusion that directly impacts the optoelectronic process by affecting the charge transport and trapping. In order to shed light on the ionic diffusion behavior, the hybrid perovskites MAPbI₃ and MAPbI₃ with minor doping of phenyl-C61-butyric acid methyl-ester (MAPbI₃-PCBM) thin-film capacitors were investigated in the presence of steady and dynamic visible illumination of different intensities. Light-induced capacitance, which increases monotonically with the increase of light intensity, was observed in the low-frequency range below 300 kHz of the electric field on both while differing quantitatively. Specifically, the large light-induced capacitance in the MAPbI₃ capacitors can be obtained in the MAPbI₃-PCBM ones in the dark. In addition, the increase of capacitance with light intensity is much less in the latter with electron trapping induced by PCBM. This result has revealed that the light-induced capacitance in MAPbI₃ capacitors can be ascribed to the contribution of the additional charges across the capacitance associated with ionic diffusion activated by the illumination and that the effects on the capacitance



will remain after the illumination is turned off due to residual photoexcited electrons trapped in the MAPbI₃-PCBM sample.

KEYWORDS: perovskites, thin film, dielectric, correlated effect, light intensity and electric field

1. INTRODUCTION

Organic-inorganic halide perovskites have several properties that make them favorable for potential applications in photovoltaics, ¹⁻³ photodetectors, ^{4,5} and other optoelectronics. These properties include long electron—hole diffusion lengths, 6,7 high absorption coefficient to visible and nearinfrared light,8 and high photoluminescence (PL) quantum efficiency. Since the first perovskite thin-film solar cells were made in 2009, the power conversion efficiency has been updated rapidly to over 22%, making them competitive to the commercially available crystalline Si, II-VI, and III-V solar cells. 10,11 However, halide perovskites are prone to instability in ambient that can be worsened by external stimuli such as humidity, heat, and light. 12 Addressing the instability issue has been a focus of intensive research recently. Progress has been made on understanding its origin and hence improving the performance of halide perovskites for practical applications.^{3,13–18} The instability of the halide perovskites originates from their intrinsic ionic solid structure, which can be affected sensitively by external environmental factors. ¹² Generally, a Goldschmidt's tolerance factor is calculated from the ratio of the ionic radii. A tolerance factor range of 0.71-1.0 is suitable for decent structural stability. 12 However, the tolerance factor may be affected by various factors both intrinsic and extrinsic. Due to the low formation enthalpy of lead halide perovskites, they can easily be formed with low-temperature fabrication

methods but on the other hand decomposed in ambient. This degradation process has been found to be accelerated by various external stimuli including light, heat, chemicals, moisture, and so forth.

In halide perovskites, it is known that ionic defects, primarily halide vacancies, can have a very small energy barrier for diffusion (e.g., 0.1–0.6 eV for I⁻ vacancies^{19–22}) even in a pristine crystal. Hence, they can diffuse and segregate readily at room temperature under a mild electric field. Furthermore, it has been observed that the defect migration rate can be enhanced by orders of magnitude under light illumination.^{21,23,24} The mechanism behind this light-enhanced diffusion behavior is still under debate.²⁵ Because ionic defects are charged particles, the segregation of these defects will have a significant impact on the electron transport. For optoelectronic devices such as solar cells, photodetectors, light-emitting diodes, and so forth, the electron transport under the convoluted influence of ion migration and light irradiation can, hence, impact the device performance directly in a

Received: March 21, 2021 Accepted: June 28, 2021 Published: July 12, 2021





complicated way. ^{17,18} For example, the photocurrent hysteresis reported in perovskite solar cells has been linked to the ion migration in perovskites. ¹⁴ The current–voltage hysteresis makes the device performance depend heavily on the precondition of the device. ^{26,27} Therefore, it is imperative to understand the mechanism behind the light-enhanced ion diffusion in order to design perovskite devices with stable and predictable performance.

In this work, we employ an Al/perovskite/FTO (FTO is for fluorine-doped tin oxide) capacitor structure to investigate the ionic diffusion behavior in the methylammonium lead iodide (MAPbI₃) perovskite thin films to understand how light illumination can impact the ion migration. Although it is established that light illumination can significantly enhance the ion diffusion rate, it is unclear whether the light affects the ionic defect motion directly by increasing the defect concentration via distorting the perovskite lattice or indirectly through the interaction between ionic defects and photoexcited carriers. It is actually challenging to distinguish the direct versus the indirect mechanisms because whenever there is light illumination, photocarriers will be produced simultaneously. To overcome this challenge, we compare the ion diffusion dynamics in plain-MAPbI3 and in MAPbI3 doped by a small amount of phenyl-C61-butyric acid methyl ester (PCBM). It is known that PCBM intercalates to/at perovskite grain boundaries. When PCBM is mixed with the halide perovskite, they form a bulk heterostructure. ^{28–30} Our recent study on perovskite/graphene photodetectors shows that PCBM can facilitate electron-hole separation and act as electron trapping sites with an extremely long electron trapping time (tens of minutes).⁵ The very long carrier trapping time allows us to study the effect of photoexcited holes/electrons on ion migration even after the light illumination is turned off. This means that the effects from the light and photocarriers can be separated. Interestingly, we have found that in the MAPbI₃-PCBM samples, ion diffusion remained fast even after the light illumination was turned off. The result shows that the residual effect of light, that is, the presence of residual photocarriers, is sufficient to enhance ion diffusion. Therefore, we propose that the light-enhanced ionic diffusion is triggered indirectly through the presence of high-concentration photocarriers.

2. EXPERIMENTAL SECTION

The perovskite MAPbI3 film was deposited on an FTO-coated glass using a one-step spin-coating method. The details of the fabrication protocol can be found in our previous works. 4,5,31 The precursor solution was prepared by dissolving lead iodide (PbI2) (Alfa Aesar, 99.9985%) and methylammonium iodide (CH3NH3I) (Luminescence Technology, 99.5%) in a stoichiometric ratio in dimethyl formamide (Sigma-Aldrich, 99.8%) with a concentration of 0.75 M. The solution was stirred at 70 °C overnight before spin coating. For the MAPbI₃-PCBM thin films, 0.1% (wt %) PCBM (Luminescence Technology, 99.5%) was mixed into the perovskite solution. PCBM was first dissolved into chlorobenzene solution. The ratio of PCBM to perovskite was controlled by mixing the required volume of PCBMchlorobenzene solution and the precursor solution. The same volume of chlorobenzene was added into the perovskite solution for preparing the perovskite reference film without PCBM. Because of the limited solubility of PCBM, the resultant solution was only fully miscible at low PCBM concentrations. The FTO-coated glass was cleaned in an ultrasonic bath with acetone and isopropyl alcohol for 15 min each and subsequently treated with ozone for an additional 15 min. The precursor solution at room temperature was spin-coated on the clean FTO-coated glass at 3000 rpm for 30 s and then 6000 rpm for 3 s

inside a N_2 -filled glove box. During the spin coating, an antisolvent, chlorobenzene (Macron), was dropped onto the film in order to facilitate the crystallization. The freshly prepared wet film was then dried on a hot plate at 60 °C for 5 min, 80 °C for 5 min, and 100 °C for 10 min in order to evaporate the residual solvent. The obtained shiny, dark brown perovskite films of thickness in the range of 265–285 nm, measured using a Tencor-P16 profiler, were allowed to cool in a N_2 environment before they were taken out for device fabrication.

On the obtained MAPbI3 and MAPbI3-PCBM films coated on FTO substrates, Al (30 nm) top electrodes were deposited using DC magnetron sputtering through a shadow mask with multiple circular holes to define the diameter of the capacitor to be 494 \pm 8 μ m with a total capacitor area of $\sim 1.9 - 2.0 \times 10^5 \,\mu\text{m}^2$. The deposition rate of Al was calibrated to be 0.54 nm/s. The dielectric properties of these perovskites thin films were investigated with capacitance-voltage (C-V) measurements using tungsten probes (Lakeshore) in a probe station in which high vacuum of about 1×10^{-6} Torr can be achieved. An Agilent semiconductor analyzer B1505A was employed for the C-V characteristic measurements. Our device can be modeled as an RC circuit consisting of a capacitor connected in parallel with a resistor of large resistance across the vertical direction through the film thickness.³² The presence of the resistance (real part of the impedance) would not prevent the ability to determine the capacitance (imaginary part of the impedance) because both quantities can be extracted from the ac measurement of the circuit impedance. The measured capacitance from which the dielectric constant, $\varepsilon \sim$ 260, can be calculated and the frequency dependence of the capacitance of our devices are anticipated for high-quality perovskites and consistent with previous reports.^{33,34} A Schott 20500 ACE 1 Fiber Optic Illuminator light source with controlled intensities of 0, 0.6, 2.9, and 6.6 mW/cm², respectively, was used to study the effect of light on the dielectric properties of MAPbI₃ and MAPbI₃-PCBM perovskite thin-film capacitors. For a better understanding of the influence light has on perovskite thin films, their capacitance was studied to show the effect of light intensity with and without PCBM doping. For all these studies, a low applied DC bias voltage of 100 mV was selected to prevent dielectric breakdown of the perovskite thin-film capacitors.3

Figure 1 shows a photograph of an array of Al/perovskite/FTO capacitors fabricated, and each capacitor has a circular shaped diameter of around 494 \pm 8 μm defined by the top Al electrodes (upper-left corner). The schematics of the MAPbI $_3$ (top) and MAPbI $_3$ -PCBM (bottom) perovskite thin-film capacitors are shown in the same figure with FTO and Al as the bottom and top electrodes, respectively. An oscillating electric field (E-field) with frequencies in

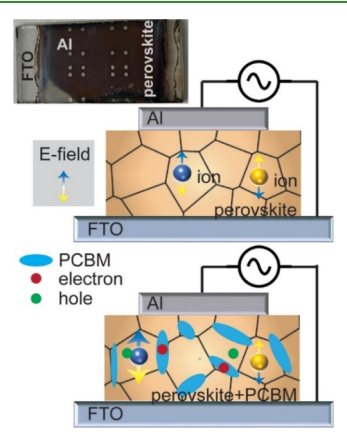


Figure 1. Photograph of an array of perovskite thin-film capacitors. Each capacitor (the silvery dot) has a circular shape with a diameter of $494 \pm 8 \ \mu m$ (upper left). The schematics show the cross section of MAPbI $_3$ (top) and MAPbI $_3$ -PCBM (bottom) capacitors. The presence of PCBM allows us to determine how photocarriers alone can affect ion diffusion in the dark.

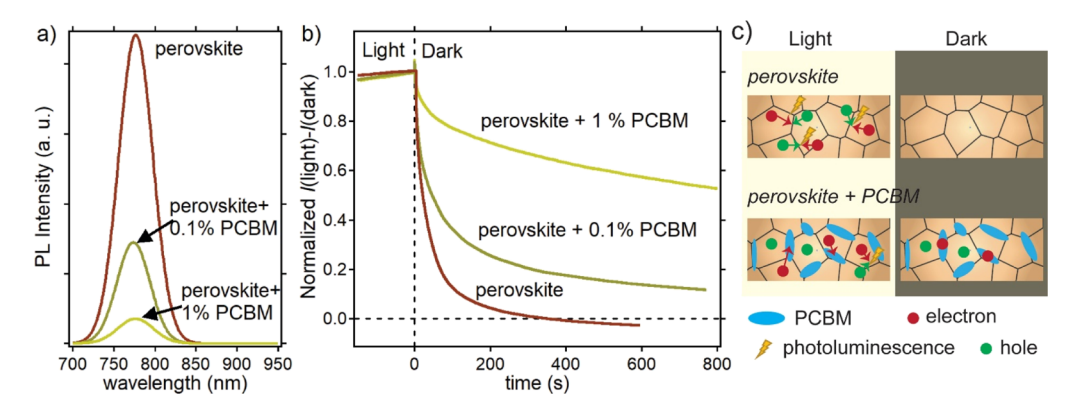


Figure 2. (a) PL spectra for the plain perovskite MAPbI₃ and the MAPbI₃-PCBM samples. (b) Decay of the photoresponse in MAPbI₃ and the MAPbI₃-PCBM on graphene devices after the light is turned off. The measurement shows that electrons are trapped in the PCBM domains for a rather long time after the light is turned off. (c) Schematic showing the effect of PCBM on the photocarriers in the MAPbI₃ and the MAPbI₃-PCBM thin films.

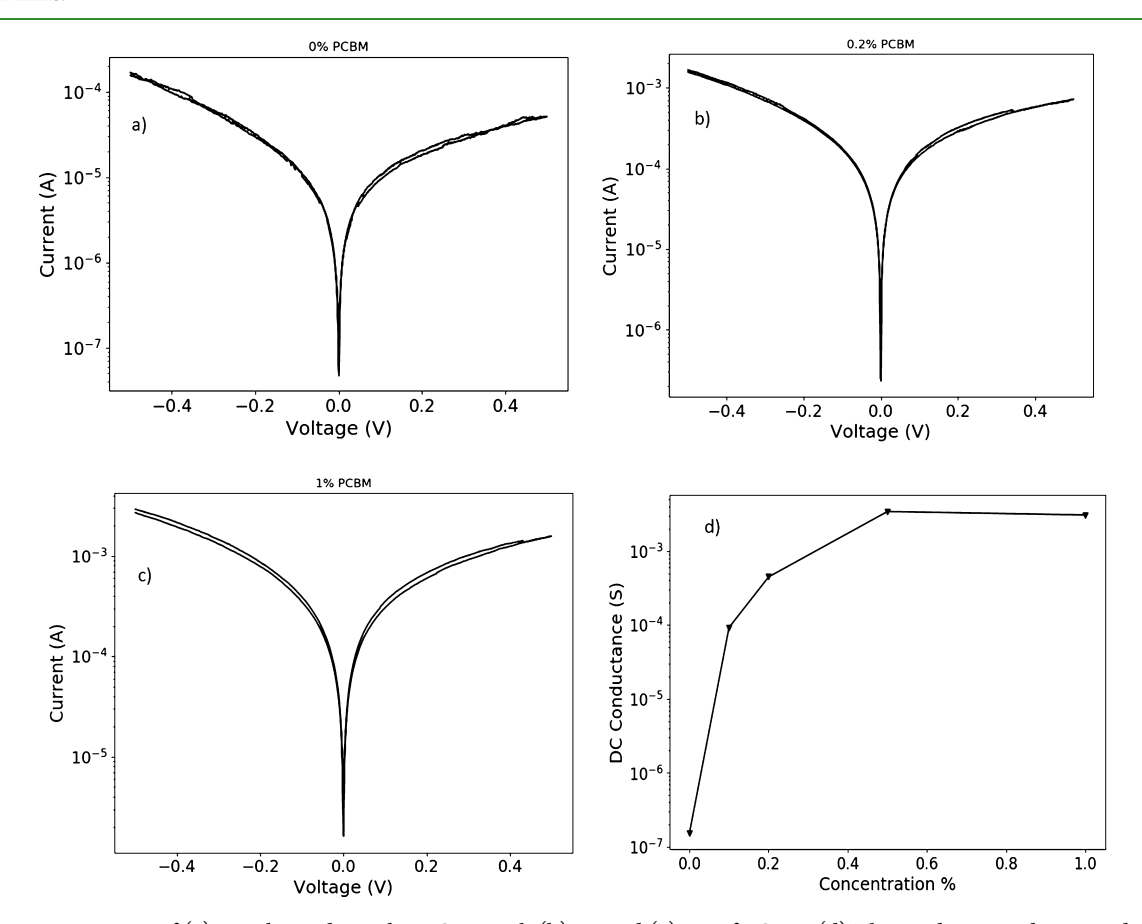


Figure 3. IV measurements of (a) MAPbI₃ and MAPbI₃-PCBM with (b) 0.2 and (c) 1% of PCBM. (d) The conductance, determined at roughly 0 V, is plotted as a function of the concentration of PCBM.

the range of 1 kHz to 1 MHz was applied across the two electrodes. The ionic polarization in the perovskite layer induced by the fast oscillating E-field can be determined from the frequency-dependent capacitance. 32,34 The experiment was done either in the dark or under continuous light illumination in order to probe the effect of light on ion diffusion. For the in-dark measurements, data was taken within 5–10 min after the light illumination was turned off. This approach allows us to study the residual effects of light illumination. The MAPbI $_3$ and MAPbI $_3$ -PCBM perovskite thin films have a similar average thickness of $\sim\!276$ nm.

As shown in our previous study, the low-concentration PCBM doping in MAPbI₃ thin films does not significantly change the thickness and morphology of the perovskite film, which can be seen in

the scanning electron microscopy (SEM) images of the pristine MAPbI₃ film and MAPbI₃-PCBM films with 0.1% and 1% PCBM doping, respectively (Figure S1 in the Supporting Information). This result is consistent with the literature, which has shown that PCBM mainly resides at perovskite grain boundaries with a negligible effect on the grain size and morphology.³⁰ However, residual photoexcited carriers can be trapped within the perovskite active layer even after the light was turned off before they recombine with electrons trapped by PCBM over a time frame of tens of minutes (bottom panel in Figure 1). Hence, it allows us to study the effect of photocarriers on the ion diffusion rate without the direct presence of light in the MAPbI₃-PCBM capacitors.

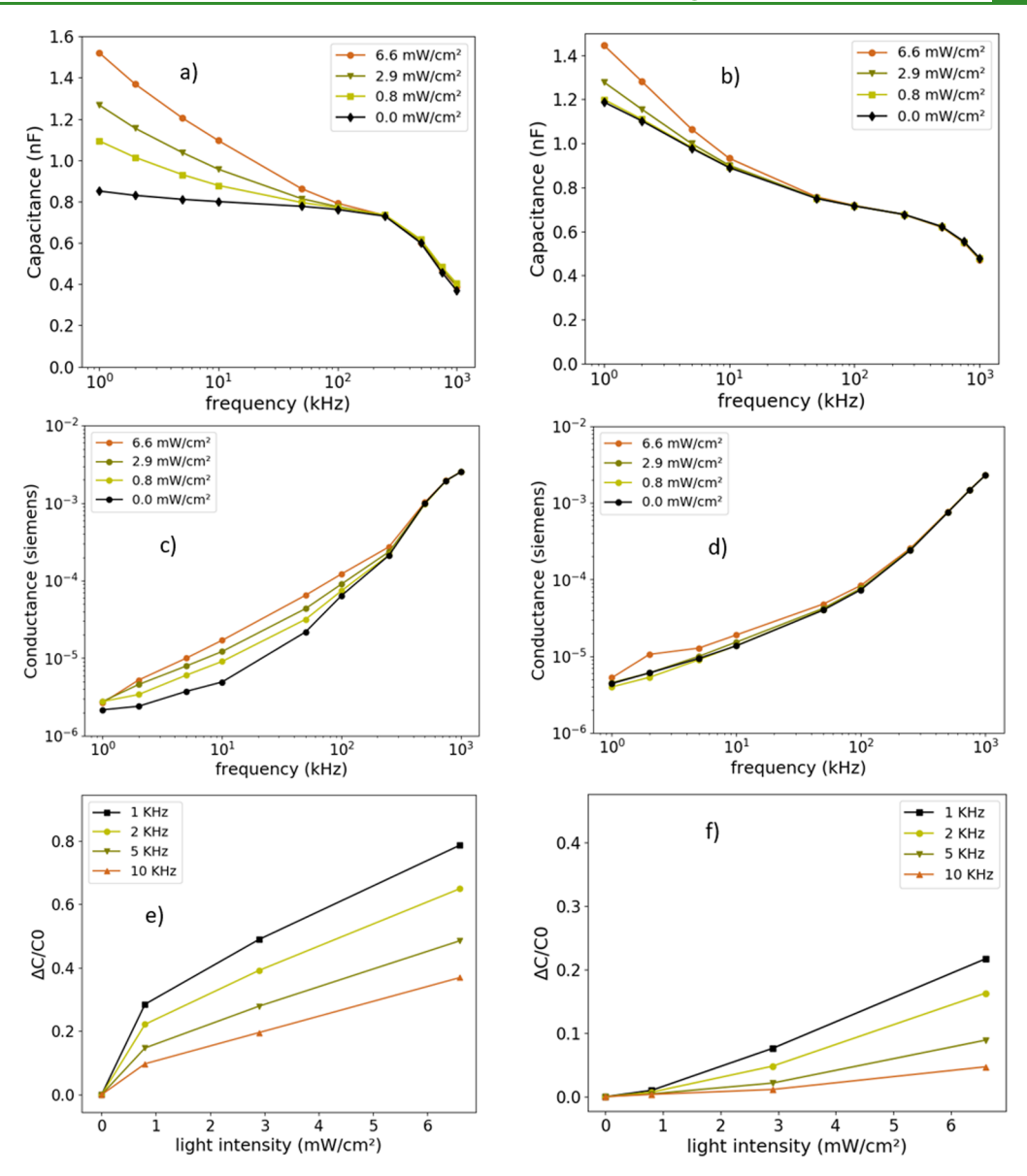


Figure 4. Variation of (a) capacitance, (c) conductance, and (e) specific change in capacitance with light intensity (0, 0.8, 2.9, and 6.6 mW/cm²) in the frequency range of 1 kHz to 1 MHz. The applied voltage was maintained at 100 mV. MAPbI₃-PCBM is shown in (b,d,f).

3. RESULTS AND DISCUSSION

The effects of PCBM on the photocarrier dynamics can be illustrated by optical spectroscopy and photodetector measurements presented in Figure 2 as detailed in our earlier studies.⁵ First, PCBM facilitates electron-hole separation when the sample is continuously illuminated by light.⁵ Figure 2a shows the comparison of the PL spectra of plain MAPbI₃, MAPbI₃-PCBM (0.1 wt %), and MAPbI₃-PCBM (1 wt %). The monotonic decrease of the PL intensity with increasing PCBM doping can be clearly seen, indicating that the PL is quenched when PCBM is added to the perovskite MAPbI₃ samples. This observation indicates that photoexcited electrons and holes are separated, or their radiative recombination is prevented in the presence of PCBM. This argument is supported in Figure 2b by the difference in response to light off in the dynamic photoresponse of MAPbI₃/graphene and MAPbI₃-PCBM/ graphene photodetectors.5,36

In these photodetectors, the perovskite layer is excited by light, and selective electron trapping in the perovskite layer,

due to the band-edge alignment at the perovskite/graphene interface, induces hole doping in graphene.^{5,36} This in turn changes the graphene conductivity via a photo-gating effect. By monitoring the change in the current (and hence conductivity) through graphene, that is, I (light) – I (dark) under a fixed bias voltage between the source and drain electrodes in Figure 2b, the amount of trapped electrons in the perovskite layer can be measured. For convenience of comparison among different devices, the amplitude of the photoresponse (I (light) - I(dark) is normalized to the initial I (light) to exhibit the decay dynamics quantitatively. Because the signal amplitude represents the amount of photoexcited electrons trapped within the MAPbI₃ photoactive layer, the signal decay time shown in Figure 2b corresponds to the trapped electron lifetime after the light illumination was turned off. With increasing PCBM doping, the lifetime increases monotonically.

The lifetime found in pristine MAPbI₃ is shorter because the charge recombination can occur promptly through radiative recombination as shown schematically in the upper panel of Figure 2c. This explanation is consistent with the stronger PL

intensity of MAPbI₃ in Figure 2a. On the other hand, for MAPbI₃-PCBM, the radiative recombination channel was prohibited due to the charge separation and electron trapping induced by PCBM (lower panel of Figure 2c), which also leads to the lower PL intensity as shown in Figure 2a. The very long lifetime of the trapped electrons in PCBM results in a residual photoresponse signal that was maintained up to tens of minutes after the light illumination was turned off. In fact, PCBM is a well-known electron acceptor. Hence, the long signal recovery time indicates that electrons (red circles in Figure 2c) are trapped by PCBM located primarily at the grain boundaries. In order to maintain charge neutrality, a MAPbI₃-PCBM film without graphene is expected to be doped by holes (green circles in Figure 2c) transiently after the light is turned off. The doping effect of PCBM is also visible in the DC conductance of the perovskite film.

Further IV measurements were conducted on MAPbI₃ films with different concentrations of PCBM. Figure 3a—c shows the IV curves for the samples with PCBM concentrations of 0, 0.2, and 1%. The obtained DC conductance is shown in Figure 3d as a function of PCBM concentration. The conductance increases monotonically as the concentration of PCBM is increased, which confirms that the MAPbI₃ perovskite film is doped by PCBM. Therefore, the long lifetime of the trapped electrons by PCBM provides us an excellent opportunity to study the ion migration in the hole-doped perovskite even after the light is turned off.

Figure 4 compares the capacitance versus frequency (C-f)of the MAPbI₃ (Figure 4a) and MAPbI₃-PCBM (0.1%) (Figure 4b) capacitors under different light intensities of 0, 0.6, 2.9, and 6.6 mW/cm², respectively. For both types of samples, the negligible effect of light on the capacitance can be observed in the high-frequency range of f > 300 kHz. The monotonic decrease of the capacitance with increasing f in this range is similar to the behavior typically found in dielectric capacitors and is often attributed to the electronic polarization of the materials. 37,38 At lower frequencies when 1/f is much larger than the electron response time, the frequency dependence of the conventional capacitance becomes negligible, which means capacitance is a constant for conventional dielectric capacitors. 33,39 However, a strong frequency dependence of the capacitance can be observed on the perovskite MAPbI3 and MAPbI₃-PCBM capacitors at lower frequencies below 300 kHz. More importantly, this capacitance increase is amplified in the presence of light in MAPbI₃ capacitors (Figure 4a). The light amplification effect becomes more pronounced at lower frequencies. Previous works^{32,34} have attributed this capacitance increase to the electrical polarization induced by the ion migration. When the frequency of the ac oscillating E-field is lower than the hopping rate of the ionic defects, these ionic charged defects can diffuse back and forth under the oscillating E-field. This can create net charge accumulation at the bottom and top surfaces of the perovskite film, which leads to an increase in capacitance.32 It was proposed that the ion migration can be speeded up by the light, which results in an amplified increase in the capacitance. Dielectric constant (ε_r) can be calculated using $\varepsilon_r = C \times d/(\varepsilon_0 A)$, where C is the measured capacitance, d is the thickness of the perovskite thin film, ε_0 is the permittivity of free space, and A is the crosssectional area of the capacitor. The highest dielectric constant of 260 was observed at the lowest frequency of 1 kHz and the highest light intensity of 6.6 mW/cm² in this study. A similar

capacitance change has been noted in other studies due to increasing voltage biasing in the dark.³⁵

In MAPbI₃-PCBM capacitors, the capacitance increases much more significantly with decreasing frequency than their MAPbI₃ counterparts even when the sample was kept in the dark. Indeed, the capacitive response of the MAPbI₃ capacitors illuminated by light (green and orange curves in Figure 4a) and the MAPbI₃-PCBM ones in the dark (black curve in Figure 4b) are essentially the same. The similarity between the two curves indicates that the capacitive response is originated from the same charged species (i.e., ionic defects). Apparently, both light illumination (Figure 4a) and PCBM addition (Figure 4b) can enhance the capacitive response originated from ionic diffusion.

As we mentioned earlier, trapped electrons in PCBM are likely to introduce p-doping in perovskites such as MAPbI $_3$ -PCBM in our study. The additional holes introduced by the electron trapping mimics the photocarriers created by light illumination. Hence, this result demonstrated experimentally that the presence of hole carriers in the perovskite can enhance the ion migration, regardless of the origin (light or PCBM) of such carriers, as predicted theoretically.

It should be noted that an increase in the overall defect concentration cannot explain the monotonic decreasing light-induced capacitance (see Figure S2 in the Supporting Information), especially when the effect of light diminishes or becomes negligible when the PCBM concentration is increased to 1.0% ($\Delta C/C_0$ in Figure S2f). This result suggests that the effect of PCBM mimics that induced by the light and both introduce doping in the perovskite. When the concentration of PCBM-induced doped carriers is comparable or even larger than the concentration of photocarriers, the effect of light on capacitance diminishes.

Several mechanisms have been proposed theoretically on how holes can enhance the halide vacancy migration. Three of the examples are as follows: (1) holes can enhance the formation of iodine vacancies; 40 (2) holes can create H+ impurity ions, which would in turn induce rearrangement of the halide ions; ⁴¹ and (3) holes can induce the formation of I²⁻ ions, which would have a lower migration barrier. 42 Although our experimental results cannot pinpoint the exact microscopic mechanism, it provides an important clue to it that the enhanced diffusion is related to the presence of hole carriers. Illuminating the MAPbI₃-PCBM sample with light can further increase the capacitance (Figure 3b), but the effect is considerably smaller especially at low light intensities when compared to the case of MAPbI₃ without PCBM doping. This means that the concentration of photocarriers at low light intensities can be small compared to that induced by the residual electrons trapped in PCBM in the MAPbI₃-PCBM sample. Hence, the effect of light on the capacitance of the MAPbI₃-PCBM sample is less apparent than in the MAPbI₃

We would also like to comment on the potential effects of the perovskite/electrode interfaces on the device capacitance. Typically, an interfacial layer with specific types of interface charges can alter the symmetry of the transport properties considerably when the electrical bias changes polarities. In the capacitors studied in this manuscript, the effect of the electrode/perovskite interfaces is unlikely significant, considering that the asymmetry of the I-V curves (Figure 3) with respect to the bias voltage polarity change is relatively small. In addition, the added PCBM at different concentrations does not

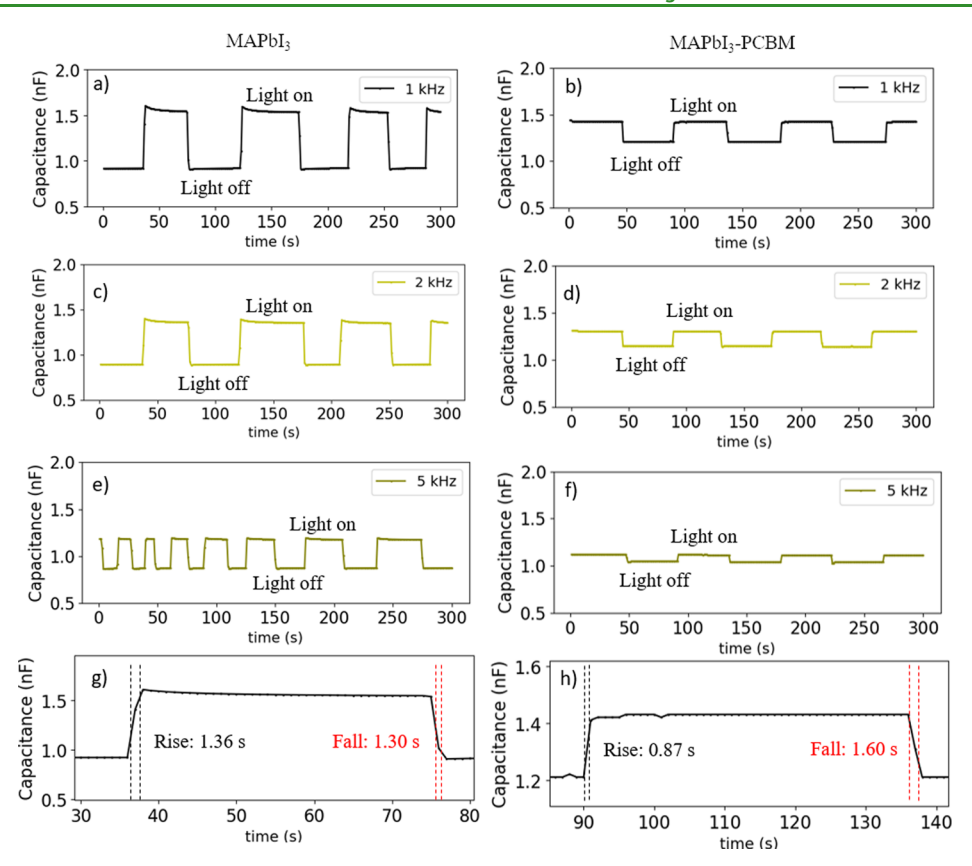


Figure 5. Dynamic capacitance variation in response to light off and on at 6.6 mW/cm² and frequency of (a) 1, (c) 2, and (e) 5 kHz for MAPbI₃ and (b) 1, (d) 2, and (f) 5 kHz for MAPbI₃-PCBM respectively. Zoomed-in views of the dynamic capacitance rise and fall between 10 and 90% of the peak height for (g) MAPbI₃ and (h) MAPbI₃-PCBM at 1 kHz. The bias voltage applied on the capacitors was maintained at 100 mV.

seem to significantly alter the symmetry of the I-V curves (Figure 3). We therefore argue that the effect of the interface does not play a dominant role in the light-induced capacitance change observed in this manuscript.

We have also monitored the ac conductance of the perovskite capacitors as a function of frequency. The result is shown in Figure 4c,d for the MAPbI3 and MAPbI3-PCBM samples, respectively. Interestingly, the conductance decreases by 2 orders of magnitude from 3×10^{-3} to 5×10^{-5} siemens in both types of samples when f is decreased from 1 MHz to 1 kHz, despite a minor difference in the effect of light illumination. Under the Drude model, the electronic conductance should increase with a decrease in f. On the other hand, the ionic conductivity often shows the opposite behavior, that is, conductance decreases with a decrease in f.43,44 Hence, our capacitance and conductance measurements in the range of 1 kHz to 1 MHz show the typical behavior of the ionic liquid. This further confirms that our measurement in the 1 kHz to 1 MHz range is probing the ion diffusion. Similar to the capacitance, the presence of either light or PCBM can increase the conductance as compared to the case of plain MAPbI₃ in the dark.

Finally, the normalized specific change in capacitance ($\Delta C/C_0$) with light intensity is shown respectively in Figure 4e for MAPbI₃ and Figure 4f for MAPbI₃-PCBM samples. We note that the curves have a convex shape for the plain MAPbI₃ capacitor but a concave shape for the MAPbI₃-PCBM one. This result is understandable under our proposed picture. For MAPbI₃, light is the dominant stimulus that can create free carriers. Hence, its effect takes off instantly and the incremental

change (the slope of the $\Delta C/C_0$ curve) is stronger at the lower light intensities. For MAPbI₃-PCBM, the perovskite is prepopulated with doped holes induced by the trapped electron in PCBM. Hence, the light effect does not show up until the concentration of carriers induced by the light is comparable to that induced by the PCBM doping.

Figure 5 compares the dynamic response of capacitance to light illumination of the MAPbI $_3$ (Figure 5a,c,e) and MAPbI $_3$ -PCBM (Figure 5b,d,f) capacitors at different frequencies of 1, 2, and 5 kHz, respectively. The time scale was varied up to 300 s to study the ion migration dynamics in the perovskite film with an applied voltage of 100 mV. For all these studies, the perovskite samples were kept inside the low vacuum of a few mTorr to prevent any further surface contamination and stored in the dark environment for \sim 5 min to ensure that the samples were in their original condition before each measurement under light illumination. The light off condition refers to dark and the light on condition refers to illumination under a light intensity of 6.6 mW/cm².

The capacitance of both MAPbI₃ and MAPbI₃-PCBM capacitors exhibits fast response to light on/off and the response is reproducible in the time frame studied. In order to quantify the response speed, the response time, defined as the time difference between 10 and 90% of the peak height of dynamic capacitance under illumination, is calculated, and the result is illustrated in Figure 5g,h for the MAPbI₃ and MAPbI₃-PCBM capacitors, respectively.

Our study shows reproducible dynamic behavior with an average "rise" time and "fall" time on the order of ~ 1 s. However, the amplitude of the dynamic capacitance change is

considerably larger in the MAPbI₃ capacitor than that of the MAPbI₃-PCBM counterpart. For example, the normalized capacitance change of the MAPbI₃ capacitor is 0.75, 0.56, and 0.36% at 1, 2, and 5 kHz, respectively, in contrast to 0.18, 0.13, and 0.07% for its MAPbI₃-PCBM counterpart. These dynamic measurements demonstrate that the ionic diffusion process is reversible under our current experimental conditions. Hence, these perovskite capacitors can be potentially used for photosensing.

4. CONCLUSIONS

In summary, we have studied the light-enhanced ionic diffusion in perovskite MAPbI3 thin-film capacitors with and without 0.1 wt % PCBM doping. The PCBM molecules serve as electron acceptors as well as trapping sites, yielding a much reduced charge recombination. Remarkably, such a charge trapping by PCBM leads to a similar light-enhanced ionic diffusion to their undoped MAPbI3 counterparts in the perovskite MAPbI3-PCBM capacitors in the dark as illustrated in the increasing capacitance with decreasing frequencies in the low-frequency range below 300 kHz. With increasing light intensities, a monotonic increase in the capacitance has been shown in both cases, while the magnitude of the increase is significantly lower in the MAPbI₃-PCBM capacitors. Dynamically, the capacitance can be tuned up and down by light on and off, and the on/off response times are approximately symmetric on the order of sub-to $\sim 1-2$ s. Our study shows that the light-enhanced ion diffusion behavior commonly observed in halide perovskites can be attributed to the presence of a high concentration of photocarriers, but not the direct effect of light to the perovskite. In this work, by using PCBM as an electron trapping site, we introduce hole doping in the perovskite, which allows us to probe the effect of holes on ion diffusion. This approach may be revised to probe the effect of electrons on ion diffusion in perovskites. Specifically, the electronaccepting PCBM may be replaced with hole-transporting polymers such as poly-triarylamin⁴⁵ or poly(N,N'-bis-4-butylphenyl-N,N'-bis(phenyl)benzidine). These polymers can selectively extract hole carriers and introduce electron doping in perovskites, allowing the effect of electron carriers on ion diffusion to be investigated.

ASSOCIATED CONTENT

Supporting Information

The Supporting Information is available free of charge at https://pubs.acs.org/doi/10.1021/acsami.1c05268.

SEM images of MAPbI₃ and MAPbI₃-PCBM with 0.1 and 1% PCBM and CV measurements of MAPbI₃ and MAPbI₃-PCBM with 0.1, 0.2, 0.5, and 1% PCBM (PDF)

AUTHOR INFORMATION

Corresponding Authors

Angelo D. Marshall — Department of Physics and Astronomy, University of Kansas, Lawrence, Kansas 66045, United States; oocid.org/0000-0003-0155-6708;

Email: angelo.marshall@ku.edu

Wai-Lun Chan – Department of Physics and Astronomy, University of Kansas, Lawrence, Kansas 66045, United

States; orcid.org/0000-0001-8697-9894;

Email: wlchan@ku.edu

Judy Z. Wu – Department of Physics and Astronomy, University of Kansas, Lawrence, Kansas 66045, United States; Email: jwu@ku.edu

Authors

Jagaran Acharya — Department of Physics and Astronomy, University of Kansas, Lawrence, Kansas 66045, United States; ⊚ orcid.org/0000-0003-1129-0974

Ghadah Alkhalifah – Department of Physics and Astronomy, University of Kansas, Lawrence, Kansas 66045, United States

Bhupal Kattel – Department of Physics and Astronomy, University of Kansas, Lawrence, Kansas 66045, United States

Complete contact information is available at: https://pubs.acs.org/10.1021/acsami.1c05268

Author Contributions

The manuscript was written through contributions of all authors. All authors have given approval to the final version of the manuscript.

Notes

The authors declare no competing financial interest.

ACKNOWLEDGMENTS

This research was supported in part by ARO contract no. ARO-W911NF-16-1-0029 and NSF contract nos. NSF-ECCS-1809293, NSF-DMR-1909292, and NSF-DMR-1508494. W.L.C. acknowledges the funding from the University of Kansas General Research Fund allocation #2151080 and from NSF DMR-1351716. G.A. acknowledges the scholarship support provided by the King Faisal University.

■ REFERENCES

- (1) Rong, Y.; Hu, Y.; Mei, A.; Tan, H.; Saidaminov, M. I.; Seok, S. I.; McGehee, M. D.; Sargent, E. H.; Han, H. Challenges for Commercializing Perovskite Solar Cells. *Science* **2018**, *361*, No. eaat8235.
- (2) Ahmadi, M.; Wu, T.; Hu, B. A Review on Organic-Inorganic Halide Perovskite Photodetectors: Device Engineering and Fundamental Physics. *Adv. Mater.* **2017**, *29*, 1605242.
- (3) Wang, K.; Jin, Z.; Liang, L.; Bian, H.; Bai, D.; Wang, H.; Zhang, J.; Wang, Q.; Liu, S. All-Inorganic Cesium Lead Iodide Perovskite Solar Cells With Stabilized Efficiency Beyond 15%. *Nat. Commun.* **2018**, *9*, 4544.
- (4) Liu, B.; Gutha, R. R.; Kattel, B.; Alamri, M.; Gong, M.; Sadeghi, S. M.; Chan, W.-L.; Wu, J. Z. Using Silver Nanoparticles-Embedded Silica Metafilms as Substrates to Enhance the Performance of Perovskite Photodetectors. *ACS Appl. Mater. Interfaces* **2019**, *11*, 32301–32309.
- (5) Qin, L.; Wu, L.; Kattel, B.; Li, C.; Zhang, Y.; Hou, Y.; Wu, J.; Chan, W.-L. Using Bulk Heterojunctions and Selective Electron Trapping to Enhance the Responsivity of Perovskite-Graphene Photodetectors. *Adv. Funct. Mater.* **2017**, *27*, 1704173.
- (6) Stranks, S. D.; Eperon, G. E.; Grancini, G.; Menelaou, C.; Alcocer, M. J. P.; Leijtens, T.; Herz, L. M.; Petrozza, A.; Snaith, H. J. Electron-Hole Diffusion Lengths Exceeding 1 Micrometer in an Organometal Trihalide Perovskite Absorber. *Science* **2013**, 342, 341–344.
- (7) Liao, Z.; Xiao, Z.; Yang, M.; Zhang, M.; Zhang, Y.; Gu, H.; Jiang, X.; Wang, Q.; Li, J. Direct Imaging of Carrier Diffusion Length in Organic-Inorganic Perovskites. *Appl. Phys. Lett.* **2019**, *115*, 242104.
- (8) De Wolf, S.; Holovsky, J.; Moon, S.-J.; Löper, P.; Niesen, B.; Ledinsky, M.; Haug, F.-J.; Yum, J.-H.; Ballif, C. Organometallic Halide

- Perovskites: Sharp Optical Absorption Edge and Its Relation to Photovoltaic Performance. J. Phys. Chem. Lett. 2014, 5, 1035–1039.
- (9) Lin, K.; Xing, J.; Quan, L. N.; de Arquer, F. P. G.; Gong, X.; Lu, J.; Xie, L.; Zhao, W.; Zhang, D.; Yan, C.; Li, W.; Liu, X.; Lu, Y.; Kirman, J.; Sargent, E. H.; Xiong, Q.; Wei, Z. Perovskite light-emitting diodes with external quantum efficiency exceeding 20 per cent. *Nature* 2018, 562, 245–248.
- (10) Kojima, A.; Teshima, K.; Shirai, Y.; Miyasaka, T. Organometal Halide Perovskites as Visible-Light Sensitizers for Photovoltaic Cells. *J. Am. Chem. Soc.* **2009**, *131*, 6050–6051.
- (11) Song, X.; Daniels, G.; Feldmann, D. M.; Gurevich, A.; Larbalestier, D. Electromagnetic, atomic structure and chemistry changes induced by Ca-doping of low-angle YBa2Cu3O7- δ grain boundaries. *Nat. Mater.* **2005**, *4*, 470–475.
- (12) Lou, S.; Xuan, T.; Wang, J. (INVITED) Stability: A Desiderated Problem for the Lead Halide Perovskites. *Opt. Mater.:* X 2019, 1, 100023.
- (13) Chen, S.; Wen, X.; Sheng, R.; Huang, S.; Deng, X.; Green, M. A.; Ho-Baillie, A. Mobile Ion Induced Slow Carrier Dynamics in Organic-Inorganic Perovskite CH3NH3PbBr3. ACS Appl. Mater. Interfaces 2016, 8, 5351–5357.
- (14) Yuan, Y.; Huang, J. Ion Migration in Organometal Trihalide Perovskite and Its Impact on Photovoltaic Efficiency and Stability. Acc. Chem. Res. 2016, 49, 286–293.
- (15) Ghosh, S.; Pal, S. K.; Karki, K. J.; Pullerits, T. Ion Migration Heals Trapping Centers in CH3NH3PbBr3 Perovskite. *ACS Energy Lett.* **2017**, *2*, 2133–2139.
- (16) Li, D.; Wu, H.; Cheng, H.-C.; Wang, G.; Huang, Y.; Duan, X. Electronic and Ionic Transport Dynamics in Organolead Halide Perovskites. ACS Nano 2016, 10, 6933–6941.
- (17) deQuilettes, D. W.; Zhang, W.; Burlakov, V. M.; Graham, D. J.; Leijtens, T.; Osherov, A.; Bulović, V.; Snaith, H. J.; Ginger, D. S.; Stranks, S. D. Photo-Induced Halide Redistribution in Organic-Inorganic Perovskite Films. *Nat. Commun.* **2016**, *7*, 11683.
- (18) Calado, P.; Telford, A. M.; Bryant, D.; Li, X.; Nelson, J.; O'Regan, B. C.; Barnes, P. R. F. Evidence for Ion Migration in Hybrid Perovskite Solar Cells With Minimal Hysteresis. *Nat. Commun.* **2016**, 7, 13831.
- (19) Eames, C.; Frost, J. M.; Barnes, P. R. F.; O'Regan, B. C.; Walsh, A.; Islam, M. S. Ionic Transport in Hybrid Lead Iodide Perovskite Solar Cells. *Nat. Commun.* **2015**, *6*, 7497.
- (20) Senocrate, A.; Moudrakovski, I.; Kim, G. Y.; Yang, T.-Y.; Gregori, G.; Grätzel, M.; Maier, J. The Nature of Ion Conduction in Methylammonium Lead Iodide: A Multimethod Approach. *Angew. Chem., Int. Ed.* **2017**, *56*, 7755–7759.
- (21) Xing, J.; Wang, Q.; Dong, Q.; Yuan, Y.; Fang, Y.; Huang, J. Ultrafast Ion Migration in Hybrid Perovskite PolycrystallineThin Films Under Light and Suppression in Single Crystals. *Phys. Chem. Chem. Phys.* **2016**, *18*, 30484–30490.
- (22) Li, C.; Guerrero, A.; Zhong, Y.; Huettner, S. Origins and Mechanisms of Hysteresis in Organometal Halide Perovskites. *J. Phys.: Condens. Matter* **2017**, *29*, 193001.
- (23) Kim, G. Y.; Senocrate, A.; Yang, T.-Y.; Gregori, G.; Grätzel, M.; Maier, J. Large Tunable Photoeffect on Ion Conduction in Halide Perovskites and Implications for Photodecomposition. *Nat. Mater.* **2018**, *17*, 445–449.
- (24) Brennan, M. C.; Draguta, S.; Kamat, P. V.; Kuno, M. Light-Induced Anion Phase Segregation in Mixed Halide Perovskites. *ACS Energy Lett.* **2018**, *3*, 204–213.
- (25) Walsh, A.; Stranks, S. D. Taking Control of Ion Transport in Halide Perovskite Solar Cells. ACS Energy Lett. 2018, 3, 1983–1990.
- (26) Domanski, K.; Roose, B.; Matsui, T.; Saliba, M.; Turren-Cruz, S.-H.; Correa-Baena, J.-P.; Carmona, C. R.; Richardson, G.; Foster, J. M.; De Angelis, F.; Ball, J. M.; Petrozza, A.; Mine, N.; Nazeeruddin, M. K.; Tress, W.; Grätzel, M.; Steiner, U.; Hagfeldt, A.; Abate, A. Migration of Cations Induces Reversible Performance Losses Over Day/Night Cycling in Perovskite Solar Cells. *Energy Environ. Sci.* 2017, 10, 604–613.

- (27) Bowring, A. R.; Bertoluzzi, L.; O'Regan, B. C.; McGehee, M. D. Reverse Bias Behavior of Halide Perovskite Solar Cells. *Adv. Energy Mater.* **2018**, *8*, 1702365.
- (28) Shao, Y.; Xiao, Z.; Bi, C.; Yuan, Y.; Huang, J. Origin and Elimination of Photocurrent Hysteresis by Fullerene Passivation in CH3NH3PbI3 Planar Heterojunction Solar Cells. *Nat. Commun.* **2014**, *5*, 5784.
- (29) Chiang, C.-H.; Wu, C.-G. Bulk Heterojunction Perovskite—PCBM Solar Cells With High Fill Factor. *Nat. Photonics* **2016**, *10*, 196–200.
- (30) Xu, J.; Buin, A.; Ip, A. H.; Li, W.; Voznyy, O.; Comin, R.; Yuan, M.; Jeon, S.; Ning, Z.; McDowell, J. J.; Kanjanaboos, P.; Sun, J.-P.; Lan, X.; Quan, L. N.; Kim, D. H.; Hill, I. G.; Maksymovych, P.; Sargent, E. H. Perovskite-Fullerene Hybrid Materials Suppress Hysteresis in Planar Diodes. *Nat. Commun.* **2015**, *6*, 7081.
- (31) Qin, L.; Kattel, B.; Kafle, T. R.; Alamri, M.; Gong, M.; Panth, M.; Hou, Y.; Wu, J.; Chan, W. L. Scalable Graphene-on-Organometal Halide Perovskite Heterostructure Fabricated by Dry Transfer. *Adv. Mater. Interfaces* **2019**, *6*, 1801419.
- (32) Wang, H.; Guerrero, A.; Bou, A.; Al-Mayouf, A. M.; Bisquert, J. Kinetic and Material Properties of Interfaces Governing Slow Response and Long Timescale Phenomena in Perovskite Solar Cells. *Energy Environ. Sci.* **2019**, *12*, 2054–2079.
- (33) Acharya, J.; Goul, R.; Romine, D.; Sakidja, R.; Wu, J. Effect of Al2O3 Seed-Layer on the Dielectric and Electrical Properties of Ultrathin MgO Films Fabricated Using In Situ Atomic Layer Deposition. ACS Appl. Mater. Interfaces 2019, 11, 30368–30375.
- (34) Zarazua, I.; Bisquert, J.; Garcia-Belmonte, G. Light-Induced Space-Charge Accumulation Zone as Photovoltaic Mechanism in Perovskite Solar Cells. *J. Phys. Chem. Lett.* **2016**, *7*, 525–528.
- (35) Bae, S.; Kim, S.; Lee, S.-W.; Cho, K. J.; Park, S.; Lee, S.; Kang, Y.; Lee, H.-S.; Kim, D. Electric-Field-Induced Degradation of Methylammonium Lead Iodide Perovskite Solar Cells. *J. Phys. Chem. Lett.* **2016**, *7*, 3091–3096.
- (36) Wu, L.; Qin, L.; Zhang, Y.; Alamri, M.; Gong, M.; Zhang, W.; Zhang, D.; Chan, W.-L.; Wu, J. Z. High-Sensitivity Light Detection via Gate Tuning of Organometallic Perovskite/PCBM Bulk Heterojunctions on Ferroelectric Pb0.92La0.08Zr0.52Ti0.48O3 Gated Graphene Field Effect Transistors. ACS Appl. Mater. Interfaces 2018, 10, 12824–12830.
- (37) Fredin, L. A.; Li, Z.; Lanagan, M. T.; Ratner, M. A.; Marks, T. J. Sustainable High Capacitance at High Frequencies: Metallic Aluminum-Polypropylene Nanocomposites. *ACS Nano* **2013**, *7*, 396–407.
- (38) Istvan Novak, J. R. M. Frequency-Dependent Characterization of Bulk and Ceramic Bypass Capacitors. 12th Topical Meeting on Electrical Performance of Electronic Packaging, 2003.
- (39) Platt, C. Encyclopedia of Electronic Components. Volume 1; O'Reilly: Farnham, 2012; Vol. 1.
- (40) Peng, C.; Chen, J.; Wang, H.; Hu, P. First-Principles Insight Into the Degradation Mechanism of CH3NH3PbI3 Perovskite: Light-Induced Defect Formation and Water Dissociation. *J. Phys. Chem. C* **2018**, *122*, 27340–27349.
- (41) Egger, D. A.; Kronik, L.; Rappe, A. M. Theory of Hydrogen Migration in Organic-Inorganic Halide Perovskites. *Angew. Chem., Int. Ed.* **2015**, *54*, 12437–12441.
- (42) Whalley, L. D.; Crespo-Otero, R.; Walsh, A. H-Center and V-Center Defects in Hybrid Halide Perovskites. *ACS Energy Lett.* **2017**, 2, 2713–2714.
- (43) Rivera, A.; León, C.; Varsamis, C. P. E.; Chryssikos, G. D.; Ngai, K. L.; Roland, C. M.; Buckley, L. J. Cation Mass Dependence of the Nearly Constant Dielectric Loss in Alkali Triborate Glasses. *Phys. Rev. Lett.* **2002**, *88*, 125902.
- (44) Khamzin, A. A.; Popov, I. I.; Nigmatullin, R. R. Correction of the Power Law of AC Conductivity in Ion-Conducting Materials Due to the Electrode Polarization Effect. *Phys. Rev. E: Stat., Nonlinear, Soft Matter Phys.* **2014**, *89*, 032303.
- (4S) Heo, J. H.; Im, S. H.; Noh, J. H.; Mandal, T. N.; Lim, C.-S.; Chang, J. A.; Lee, Y. H.; Kim, H.-j.; Sarkar, A.; Nazeeruddin, M. K.;

Grätzel, M.; Seok, S. I. Efficient Inorganic—Organic Hybrid Heterojunction Solar Cells Containing Perovskite Compound and Polymeric Hole Conductors. *Nat. Photonics* **2013**, *7*, 486—491. (46) Zhao, D.; Sexton, M.; Park, H.-Y.; Baure, G.; Nino, J. C.; So, F. High-Efficiency Solution-Processed Planar Perovskite Solar Cells with a Polymer Hole Transport Layer. *Adv. Energy Mater.* **2015**, *5*, 1401855.